Coastal Engineering 80 (2013) 137–147

Contents lists available at SciVerse ScienceDirect

Coastal Engineering

journal homepage: www.elsevier.com/locate/coastaleng

# Wave loads on rubble mound breakwater crown walls in deep and shallow water wave conditions

Jørgen Quvang Harck Nørgaard *, Thomas Lykke Andersen, Hans F. Burcharth

*Department of Civil Engineering, Aalborg University, Sohngaardsholmsvej 57, DK-9000, Denmark*

ARTICLE INFO

*Article history:*
Received 13 March 2013
Received in revised form 28 May 2013
Accepted 2 June 2013
Available online 8 July 2013

*Keywords:*
Rubble-mound breakwater
Crown-wall
Superstructure
Wave loads
Wave height distribution

ABSTRACT

The semi-empirical formulae by Pedersen (1996) for wave loads on vertical front faces of stiff crown walls are based on model tests with deep and intermediate water wave conditions. A new series of model tests performed at the same test facility as used by Pedersen has revealed that the formulae by Pedersen overpredict the loads in shallow water wave conditions. This paper presents a modification/expansion of the formulae to cover loads in both deep and shallow water wave conditions. The modification is based on a series of 162 physical model tests on typical rubble mound breakwaters with crown wall superstructures. The implementation of shallow water wave conditions in the formulae is done by modifying the term for wave run-up to be dependent on the incident wave height distribution. Moreover, the adjusted formulae provide more accurate estimates of the wave loads on free walls without front armour protection. Pressure transducers with very high eigen-frequencies were used in the present model tests as opposed to the transducers applied by Pedersen which in some cases seem to have been affected by dynamic amplifications.



## 1. Introduction

Crown wall structures are typically used for protecting access roads against excess overtopping discharges. Fig. 1 illustrates typical rubble mound breakwater cross sections with superstructures.

The wave induced loads on the wall front and on the base plate must be known for determination of the overall stability of the superstructure and the stresses in the structure elements. Günback and Ergin (1983) linked the determination of the wave loads to a fictive run-up height. However, the concept was not further explored by the authors due to lack of physical model test results.

The concept of Günback and Ergin was, in a slightly modified form, adopted by Pedersen (1996) who on the basis of 373 physical model tests in a wave flume at Aalborg University, Denmark, derived formulae for wave induced horizontal loadings and related overturning moments on stiff crown wall superstructures. Various breakwater front slopes and degrees of armour protection of the wall were evaluated in the tests.

The formulae by Pedersen (1996) are included in the Coastal Engineering Manual (U.S. Army Corps of Engineers, 2002). However, the tests and the formulae by Pedersen are limited to deep to intermediate water wave conditions and are therefore not validated for depth limited design conditions which are present at many sites ($H_{m0}/h > 0.2$). $H_{m0}$ is the significant wave height based on frequency domain analysis and $h$ is the water depth.

Martin et al. (1999) applied also the concept proposed by Günback and Ergin and derived on the basis of small-scale model tests a set of formulae for horizontal and vertical wave pressures on stiff crown walls. The method was compared to results from laboratory tests by Burcharth et al. (1995) and Jensen (1984), and fairly good agreement was obtained. The formulae by Martin et al. (1999) are based on tests with monochromatic waves and not irregular random waves.

The following paragraphs present a new set of physical model tests for the determination of the wave induced loadings on wave wall superstructures in deep and shallow water wave conditions. The test results are compared to predictions by the formulae of Pedersen (1996) and Martin et al. (1999). The Pedersen (1996) formulae are selected for upgrading in order to cover the results of the present model tests. The modified formulae are then evaluated against the present model test results, and it is demonstrated that the modified formulae predict horizontal wave induced loadings and related tilting moments for shallow water wave conditions significantly better than the original formulae.

## 2. Model test setup

Physical tests were performed in a 1.5 m wide and 25 m long wave flume at Aalborg University, as shown in Fig. 2. Three resistance type wave gauges were installed near the toe of the breakwater to separate incident and reflected waves using the approach of Mansard and

* Corresponding author. Tel.: +45 248 46077.
*E-mail addresses:* jhn@civil.aau.dk (J.Q.H. Nørgaard), tla@civil.aau.dk (T.L. Andersen), hansburcharth@gmail.com (H.F. Burcharth).

0378-3839/$ – see front matter © 2013 Elsevier B.V. All rights reserved.
http://dx.doi.org/10.1016/j.coastaleng.2013.06.003

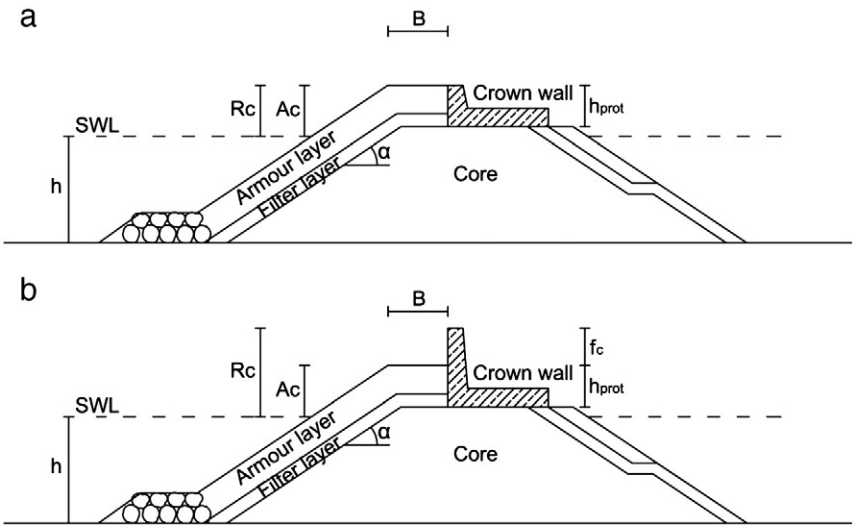


**Fig. 1.** a) Crown wall with vertical face protected by armour units. b) Crown wall with partly protected and partly un-protected vertical faces.

Funke (1980). The positioning of the wave gauges is based on the suggestions by Klopman and van der Meer (1999).

### 2.1. Rubble mound materials and structure geometries

All materials are quarried rock. The sizes are given in Table 1. The armour material is slightly over-sized in order to remain stable in all tests.

Tested ranges of structure dimensions are given in Table 2. Modifications are performed on the structure by raising the unprotected wall height, $f_c$, and for each modification the range of wave conditions in Table 2 was repeated. The symbols in Table 2 are illustrated in Fig. 1.

### 2.2. Pressure transducer instrumentation

Pressure transducers of model series Drück PMP UNIK with diameter 20 mm and correct frequency response up to 5 kHz was used for determining wave pressures on the superstructure. The transducers were mounted flush with the structure wall face. All pressures were measured relative to the atmospheric pressure. Prior to the experiments, it was verified that the transducers did not suffer from temperature drift and nonlinearity.

Solely horizontal wave loads are considered in the present paper. However, since results are further interpreted in the study by Nørgaard et al. (2012), concerning the overall stability of the crown wall, both horizontal and vertical pressure transducers are installed in the model. Moreover, the correlation of maximum horizontal and vertical loads will be considered in the present paper. By following the same approach as in Lamberti et al. (2011) signals from the sensors were sampled with 1.5 kHz and hereafter digitally low-pass filtered to obtain an appropriate sampling frequency corresponding to the spatial resolution of the transducers and the celerity of the peak pressures. A cut-off frequency of 250 Hz was applied.

The geometry of the crown wall and positioning of the pressure transducers are shown in Fig. 3. The crown wall models were made from stiff aluminium plates fixed to the walls of the flume in order to avoid influence from structural deformations when measuring the impulsive wave induced load peaks. Attachable sections were applied on top of the vertical front face in order to upgrade the crown wall height during the tests.

Photos of the shallow water test setup are shown in Fig. 4. One of the attachable sections mounted with pressure transducers on the crown wall is shown in Fig. 4 (left). A photo of the pressure transducers on the rear side of the wall is shown in Fig. 4 (right). A wire mesh screen was mounted in front of the pressure transducers on the rock covered part of the crown wall in order to protect the transducer membranes from impacting rocks.

## 3. Wave conditions

Waves were generated from a hydraulically driven piston mode generator controlled by the software AwaSys (Aalborg University, 2010). Simultaneously, active absorption of reflected waves was used in all tests. The wave generation is based on the JONSWAP spectrum, which is a three-parameter spectrum defined by $H_{m0}$, $f_p$ ($=1/T_p$), and the peak enhancement factor was chosen to be $\gamma = 3.3$ in all tests. 1250 waves were generated in each test. The tests were performed in deep and shallow water wave conditions within the target ranges given in Table 3.

## 4. Horizontal wave pressure integration

Each horizontal row contains two or three pressure gauges, see Fig. 3. The average pressure recorded in each horizontal row is used in the integration procedure given below. The nominations of these pressures are shown in Fig. 5.

$H_0$ and $H_5$, in Fig. 5a) and $H_0$ and $H_6$ in Fig. 5b) are not measured directly but are obtained by linear extrapolation of the neighbouring measured pressures, however, with a minimum of 0 kPa. An example for calculation of $H_0$ and $H_6$ in Fig. 5b) is given in Eq. (1).

$$H_0 = H_1 - \frac{(H_2 - H_1)}{h_2} h_1, \quad H_6 = H_5 - \frac{(H_4 - H_5)}{h_5} h_6 \tag{1}$$

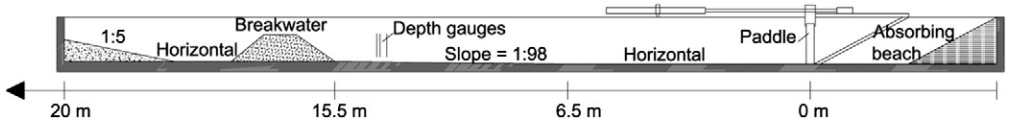


**Fig. 2.** Layout of model test in 2D wave flume.

**Table 1**
Material sizes used in the rubble mound breakwater model.

| Core material | Filter material | Armour material |
|---|---|---|
| $D_{n50} = 5$ mm | $D_{n50} = 20$ mm | $D_{n50} = 40$ mm |

The wave induced horizontal force $F_H$ and the corresponding moment $M_{FH}$ around the toe of the vertical wall in Fig. 5b) are determined using Eq. (2). Piecewise linear trapezoidal pressure distributions are assumed between the measured pressures due to the relatively short distances between the individual transducers.

$$\begin{aligned}
&\Delta F_{H,hn} = \frac{1}{2} h_n (H_{n-1} + H_n) \\
&F_H = \sum_{n=1}^{n=6} \Delta F_{H,hn} \\
&\Delta M_{F_{H,hn}} = \frac{1}{2} h_n \left[ h_n \left( \frac{1}{3} H_{n-1} + \frac{2}{3} H_n \right) + (H_{n-1} + H_n) \sum_{i=1}^{n-1} h_i \right] \\
&M^O_{F_H} = \sum_{n=1}^{n=6} \Delta M_{F_{H,hn}}
\end{aligned} \tag{2}$$

As an example, the measured pressure distribution is plotted in Fig. 6 at the instance of maximum horizontal wave force during a specific test series. 0.1%-exceedance values are determined based on linear interpolation between measured values with higher and lower exceedance probabilities.

## 5. Evaluation of existing design formulae

### 5.1. Design load formulae by Pedersen (1996)

The distribution of wave induced pressure and the related resultant wave forces on a crown wall are illustrated in Fig. 7.

One of the governing terms in the formulae by Pedersen (1996) is the fictive wave run-up height exceeded by 0.1% of the incoming waves, $R_{u,0.1\%}$. Pedersen derived the wave loads on a plain wall based on the run-up wedge and design parameters given in Fig. 8 (right). Pedersen used the Van der Meer and Stam (1992) run-up formula for deep-water wave conditions with head-on wave attack and non-overtopped rough straight slopes given by Eq. (3) when fitting his formulae to the model test results. $H_{1/3}$ is the time domain incident significant wave height at the toe of the structure and $\alpha$ is the breakwater front-slope. For the surf similarity parameter, $\xi_m$, the mean wave period, $T_m$, is used.

$$R_{u,0.1\%} = \begin{cases} 1.12 H_{1/3} \xi_{m0} & \xi_{m0} \le 1.5 \\ 1.34 H_{1/3} \xi_{m0}^{0.55} & \xi_{m0} > 1.5 \end{cases}, \quad \xi_{m0} = \frac{\tan\alpha}{\sqrt{\frac{2\pi}{g} \cdot \frac{H_{1/3}}{T_m^2}}} \tag{3}$$

The formula by Van der Meer and Stam (1992) is only valid for relatively deep water and has a maximum of $R_{u,0.1\%}/H_{1/3} \le 2.58$.

Pedersen suggested that other run-up formulae might have been applied. This, however, would possibly change the empirical scale factors used for the calibration due to the bias in the run-up formulae. The calibration of scale factors is discussed later.

Pedersen (1996) assumed a vertical pressure distribution as shown in Fig. 8 (left). The related resulting forces on the upper unprotected and the lower protected parts of the wall are denoted $F_{Hu}$ and $F_{Hl}$, respectively.

The height of the upper wave impact zone, $y_{eff}$, is given by:

$$y_{eff} = \min\left[\frac{y}{2}; f_c\right] \tag{4}$$

$y$ is the vertical run-up wedge thickness and $f_c$ is the vertical distance from the armour crest to the top of the crown wall face. The resultant wave forces on the upper and lower parts of the crown wall are given by Eq. (5).

$$\begin{aligned}
&F_{Hu,0.1\%} = a \cdot \sqrt{\frac{L_{m0}}{B}} \cdot p_m \cdot y_{eff} \cdot b \\
&F_{Hl,0.1\%} = \frac{1}{2} \cdot a \cdot \sqrt{\frac{L_{m0}}{B}} \cdot p_m \cdot V \cdot h_{prot} \\
&p_m = g \cdot \rho_w \cdot \left( R_{u,0.1\%} - A_c \right) \\
&V = \begin{cases} \frac{V_2}{V_1} & \text{for } V_2 < V_1 \\ 1 & \text{for } V_2 \ge V_1 \end{cases}
\end{aligned} \tag{5}$$

$a = 0.21$ and $b = 1.6$ are empirical scale factors calibrated from the 373 tests by Pedersen (1996). $A_c$, $B$, $h_{prot}$, and the volumes $V_1$ and $V_2$ are defined in Fig. 8 (right). $L_{m0} = g \cdot T_m^2 / 2\Pi$ is the deep water wave length based on the spectral mean period, $\rho_w$ is the mass density of water, and $g$ is the local gravitational acceleration.

The 0.1% exceedance values of the total horizontal force, the related moment around the bottom of the wall, and the pressure at the wall-base corner are given by Eq. (6). $c = 0.55$ and $d = 1$ are empirical constants.

$$\begin{aligned}
&F_{H,0.1\%} = F_{Hu,0.1\%} + F_{Hl,0.1\%} = a \cdot \sqrt{\frac{L_{m0}}{B}} \cdot \left( p_m \cdot y_{eff} \cdot b + \frac{p_m}{2} \cdot V \cdot h_{prot} \right) \\
&M_{H,0.1\%} = c \cdot \left( h_{prot} + y_{eff} \right) \cdot F_{H,0.1\%} \\
&P_{b,0.1\%} = d \cdot V \cdot p_m
\end{aligned} \tag{6}$$

It should be mentioned, that $F_{H,0.1\%}$, $M_{H,0.1\%}$, and $p_{b,0.1\%}$ are not necessarily occurring at the same time. Most importantly $F_{H,0.1\%}$ and $p_{b,0.1\%}$ are not occurring simultaneously, for which reason it is conservative in stability calculations to assume the horizontal force occurring simultaneously with the generally used triangular uplift force calculated on the basis of the base front corner pressure. The formulae (Eq. (6)) are validated by Pedersen to the ranges given in Table 4.

### 5.2. Comparison of present model test results with predictions by the Pedersen (1996) formulae

The results of the present model tests are shown in Fig. 9 compared to results predicted by the Pedersen formulae. Deviations are given in terms of the sample standard error $S_e$ defined by Eq. (7). The plotted results include both deep water wave conditions ($H_{m0}/h \le 0.2$) and intermediate to shallow water wave conditions ($H_{m0}/h > 0.2$) with protected vertical wall ($f_c = 0$) and with unprotected vertical wall ($f_c > 0$), see the definitions in Fig. 8 (right). The calculated wave loads in Fig. 9 are based on the calibration factors from the original design formulae by Pedersen (1996).

**Table 2**
Ranges of structure dimensions for the breakwater model.

| Test series | $R_c$ [m] | $A_c$ [m] | $\alpha$ [–] | $B$ [m] | $R_c/A_c$ [–] | $A_c/B$ [–] | $f_c/A_c$ [–] |
|---|---|---|---|---|---|---|---|
| Shallow water | 0.20–0.29 | 0.20–0.24 | 1:1.5 | 0.24 | 1.00–1.33 | 0.83–1.00 | 0–0.35 |
| Deep water | 0.1–0.19 | 0.1–0.14 | 1:1.5 | 0.17 | 1.00–1.70 | 0.59–0.82 | 0–0.70 |

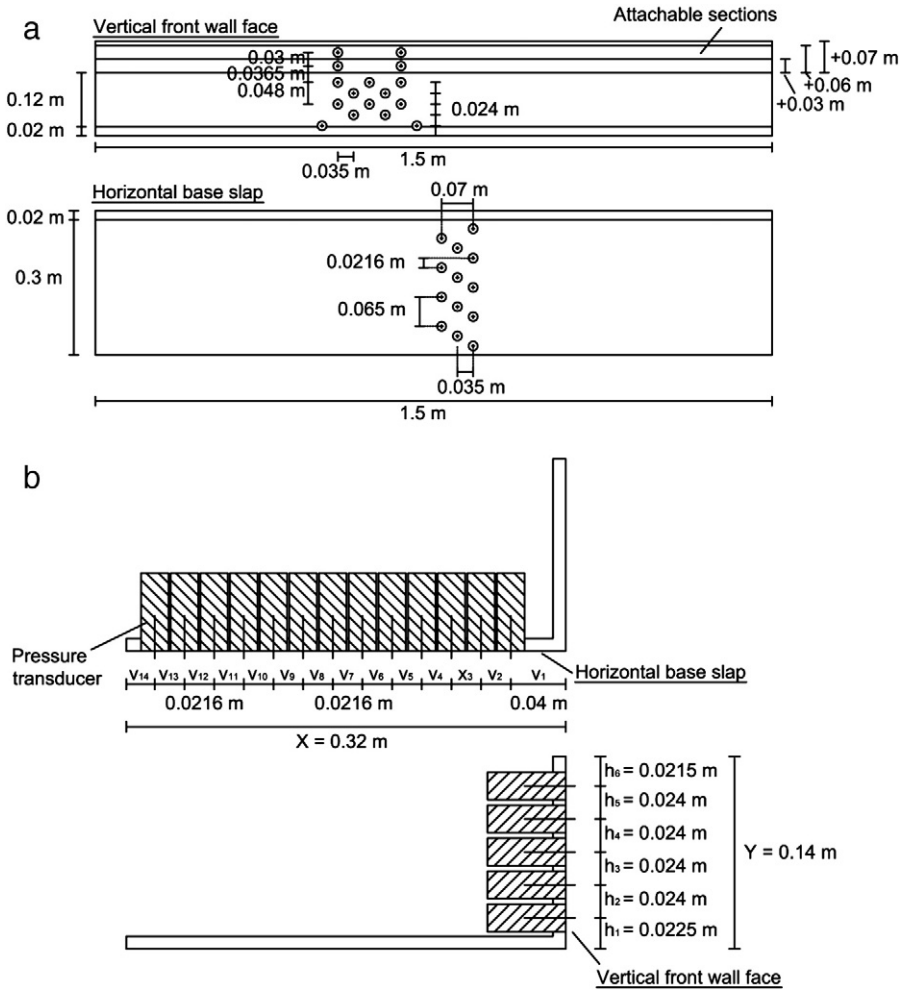


**Fig. 3.** a) Positioning of pressure transducers on the front face of the shallow water breakwater model with attachable sections. b) Cross-sectional illustration of crown wall model without attachable sections.

$$S_e = \sqrt{\frac{1}{\nu}\sum_{i=1}^{n}(meas_i - calc_i)^2} \qquad \nu = n-2 \tag{7}$$

$n$ is the number of values, $meas_i$ are the measured values, and $calc_i$ are the calculated estimates of $meas_i$.

As seen from Fig. 9, the design formulae by Pedersen (1996) are performing well in deep water wave conditions with $f_c = 0$. However, when evaluating the test results from the shallow water wave conditions, the wave loads are highly overestimated by the existing design formulae. Moreover, it can be concluded that the formulae overestimate the wave loads for $f_c > 0$ in both deep water wave conditions and shallow water wave conditions.

### 5.3. Design load formulae by Martin et al. (1999)

The formulae by Martin et al. (1999) are based on model tests in a scale of 1:90 in a 2 m wide, 2 m high and 70 m long wave flume at the Ocean and Coastal Engineering Laboratory at the University of

**Fig. 4.** (Left) Front view of attachable sections with pressure transducers for raising the unprotected crown wall height. (Right) Pressure transducers on the rear side of the wall.

**Table 3**
Ranges of target conditions in deep water and shallow water wave test series.

| Test series | $h$ [m] | $H_{m0}$ [m] | $T_{m-1,0}$ [s] | $H_{m0}/h$ [−] | $A_c/H_{m0}$ [−] |
|---|---|---|---|---|---|
| Shallow water | 0.300–0.360 | 0.150–0.180 | 1.826 | 0.500 | 1.00–1.600 |
| Deep water | 0.500–0.560 | 0.100 | 1.826 | 0.179–0.200 | 0.800–1.400 |

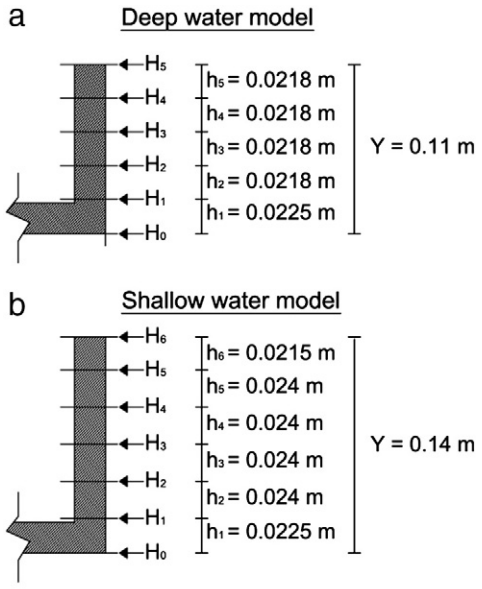


**Fig. 5.** Illustration of horizontal pressures on the crown-wall.

Cantabria. The tested cross section was a model of the Spanish Príncipe de Asturias breakwater in Port of Gijón (illustrated in Fig. 10). Vertical and horizontal wave pressures were measured from four strain-gauge type pressure gauges under the base slap and eight gauges on the vertical front face. Pressures were acquired with a sampling rate of 150 Hz and integrated by a rectangular method. Prototype parallelepiped concrete blocks of 90 t (core) and 120 t (armour) were modelled in the tests, resulting in much larger permeability than in normal rubble mound breakwaters. The tests were performed with regular waves.

The formulae by Martin et al. (1999) describe two different peaks in the pressure evolution: the dynamic pressure peak, which is usually the largest peak but with a short duration, and the reflective pressure peak which lasts longer. Both pressure peaks are related to the berm width, $B$, and berm height, $A_c$. Moreover, the peaks are related to three parameters; $a$, $\mu$ and $\lambda$, which are calibrated from the tests and depend on the wave steepness, $H/L$, the relative berm width, $B/L$, and the number of armour units on the berm. The wave steepness range in the tests was $0.03 < H/L < 0.075$ at the breakwater toe.

The dynamic peak pressure $P_{s0}$ by Martin et al. (1999) at the berm crest level, $z = A_c$ c.f. Fig. 11, is given in Eq. (8) where $a$ is a non-dimensional empirical parameter. The dynamic pressure as function of $z$ is given in Eq. (9). $\lambda$ is an empirical non-dimensional parameter based on the ratio of the berm width and the local wave length $B/L$. $P_r$ in Fig. 11 is the reflective peak pressure, given in Eq. (10), which occurs immediately after the dynamic pressure peak. $m$ in Eq. (10) is a dimensionless parameter, which was evaluated experimentally based on monochromatic waves. Martin et al. (1999) derived the parameters $a = 0.296$, $b = 0.073$, and $c = 383.1$ for three armour units on the berm, however, for relatively large units and a porous core.

$$P_{S0} = a\cdot\rho_w\cdot g\cdot S_0,\quad S_0 = H\left(1-\frac{A_c}{R_u}\right),\quad a = 2.9\left(\frac{R_u}{H}\cos\alpha\right)^2 \tag{8}$$

$$P_d(z) = \begin{cases} P_{S0} & \text{for } z > A_c \\ \lambda P_{S0} & \text{for } w_f < z < A_c \end{cases} \tag{9}$$
$$\lambda = 0.8\cdot e^{-10.9\cdot\frac{B}{L}}$$

$$P_r(z) = m\cdot\rho_w\cdot g(S_0 + A_c - z)\quad \text{for } w_f < z < A_c + S_0 \tag{10}$$
$$m = a\cdot e^{c(H/L-b)^2}$$

The wave run-up height by Martin et al. (1999) in Eq. (11) is based on the surf similarity parameter on deep water, $\xi_0$, and two empirical coefficients, $A_u$ and $B_u$, which depend on the type of armour unit.

$$\frac{R_u}{H} = A_u\left(1-e^{B_u\cdot\xi_0}\right),\quad \xi_0 = \frac{\tan\alpha}{\sqrt{\frac{2\pi}{g}\cdot\frac{H}{T^2}}} \tag{11}$$

Martin et al. (1999) suggest extending the method to random irregular waves by performing zero crossing to obtain individual $H$ and $T$ from a synthetic surface elevation time series based on e.g. a TMA spectrum with $H_s$, $T_z$, and a spectral shape parameter as input. The breaking criterion by Miche is suggested to be applied to each individual wave in the time series.

### 5.4. Comparison of the present test results with predictions by the formulae by Martin et al. (1999)

Results from the present tests are compared to the estimations from the formulae by Martin et al. (1999) in Fig. 12. Measured values of $H_{max}$ and $T_{H,max}$ are used as regular wave input in the formulae to obtain maximum wave loads instead of generating synthetic time series. $A_u = 1.2$ and $B_u = -0.7$, which are best fit values from

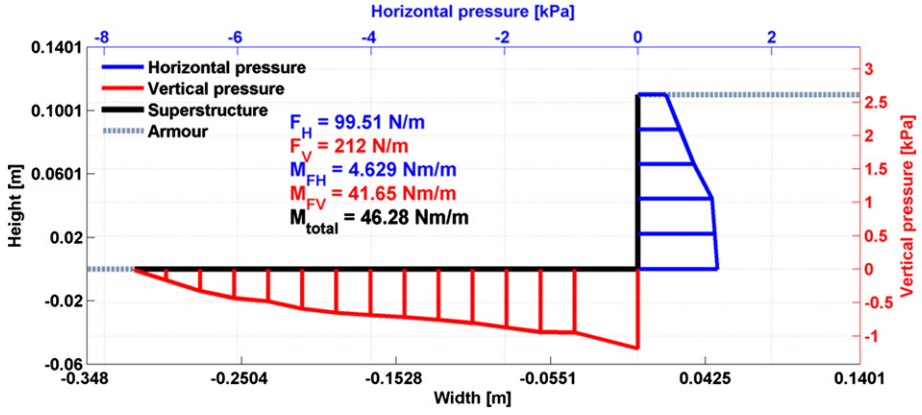


**Fig. 6.** Example of integrated wave induced pressure on superstructure at the instance of maximum horizontal wave induced load.

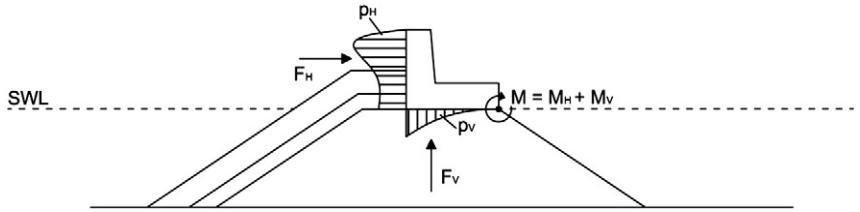


**Fig. 7.** Definition of wave induced pressure and resultant forces on rubble mound structures. Redrawn from Pedersen (1996).

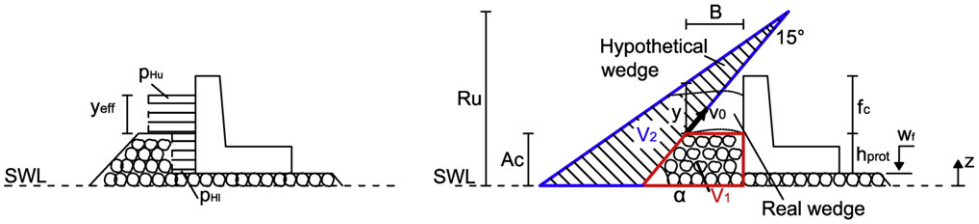


**Fig. 8.** (Left) Assumed pressure distribution on crown wall. (Right) Run-up wedge and design parameters. Redrawn from Pedersen (1996).

Martin et al. (1999), are used in the estimations. Despite using five armour units on the berm in the present tests the parameters *a*, *b*, and *c* for three units are applied in Eq. (10), since this is the best available. The horizontal overturning moment $M_{H,0.1\%}$ is determined from the spatial pressure distribution on the vertical crown wall face, illustrated in Fig. 11.

It is seen from Fig. 12 that $F_{H,0.1\%}$, $M_{H,0.1\%}$, and $P_{b,0.1\%}$ are generally relatively well predicted by the formulae of Martin et al. (1999), although some scatter is present. The tendency is, however, that the largest values of $F_{H,0.1\%}$ and $M_{H,0.1\%}$ on the wall are overestimated and the largest values of $P_{b,0.1\%}$ are underestimated. Since the maximum wave height $H_{max}$ is used directly in the formulae by Martin et al. (1999), the effects of shallow water wave height distribution seem to be included. Additionally, the formulae are performing relatively well also on the unprotected wall face.

## 6. Selection of design formulae for modification/calibration to the present tests

When comparing the performances of the design formulae by Pedersen (1996) and Martin et al. (1999) in Figs. 9 and 12, respectively, the formulae by Martin et al. (1999), as a starting point, provide the best overall estimates for all considered $H_{m0}/h$ ratios. However, if comparing the formulae by separating into deep and shallow water wave conditions, the formulae by Pedersen (1996) provide the best load model when $H_{m0}/h \leq 0.2$ and $f_c = 0$. Moreover, from the comparison of measured and estimated values of $P_{b,0.1\%}$ and $M_{H,0.1\%}$, it is seen that the spatial pressure distribution is better modelled by Pedersen (1996). Based on this, the formulae by Pedersen (1996) will be modified in the following to include the effects of shallow water wave conditions and will be upgraded to perform better on the un-protected wall face, $f_c > 0$.

**Table 4**
Parameter validity ranges for the formulae (Eq. (6)) by Pedersen (1996).

| Parameter | Range |
|---|---|
| $\xi_m$ | 1.1–5.2 |
| $H_{m0}/A_c$ | 0.5–1.5 |
| $R_c/A_c$ | 0.3–1.1 |
| $A_c/B$ | 1–2.6 |
| $\cos\alpha$ | 1.5–3.5 |
| $H_{m0}/h$ | 0.16–0.35 |

Moreover, the expression for the overturning moment will be modified to have a physical relation with the assumed spatial pressure distribution instead of the relation in Eq. (6). The formulae by Martin et al. (1999) are not considered any further in the present paper.

## 7. Update of design formulae by Pedersen (1996)

### 7.1. Modification to include shallow water wave conditions

It is generally accepted that the wave height distribution for wind generated deep water waves follows the Rayleigh-distribution function. Moreover, Kobayashi et al. (2008) have shown that if the incident irregular wave heights are Rayleigh-distributed then the wave run-up heights on a structure can also be assumed to be Rayleigh-distributed. Eq. (3) is based on tests in deep water where Rayleigh distributed wave heights and run-up heights can be assumed. If it is assumed that, in general, the run-up height distribution follows the wave height distribution then $H_{0.1\%}$ should be the parameter for $R_{u,0.1\%}$ in Eq. (3) instead of $H_{1/3}$. Since according to the Rayleigh distribution $H_{1/3}/H_{0.1\%} = 0.538$ then Eq. (3) is adjusted to Eq. (11).

$$R_{u,0.1\%} = \begin{cases} 0.603 H_{0.1\%} \xi_{m0} & \xi_{m0} \leq 1.5 \\ 0.722 H_{0.1\%} \xi_{m0}^{0.55} & \xi_{m0} > 1.5 \end{cases} \quad (12)$$

If no information is available $H_{0.1\%}$ can be estimated from an appropriate wave height distribution valid also for shallow water wave conditions, e.g. distribution by Battjes and Groenendijk (2000) based on the spectral significant wave height, $H_{m0}$, water depth, and the sea bed slope. In Fig. 13, the measured values of $H_{0.1\%}$ in the present data set are compared to the Rayleigh-distribution and the Battjes and Groenendijk (2000) distribution. As expected, the Rayleigh-distribution overestimates $H_{0.1\%}$ in shallow water wave conditions, $H_{m0}/h > 0.2$, whereas the prediction, by the method of Battjes and Groenendijk, corresponds very well to the measured values in both deep and shallow water wave conditions.

Fig. 14 shows the performance of the Pedersen formulae when the run-up formula (11) is applied for the condition of $f_c = 0$. For $H_{0.1\%}$ are used measured values from the present tests. Very good agreement between measured values from the present tests and calculated values is obtained, which indicates that the Pedersen (1996) formulae can be applied for shallow water wave conditions, if using an appropriate model for the wave run-up height.

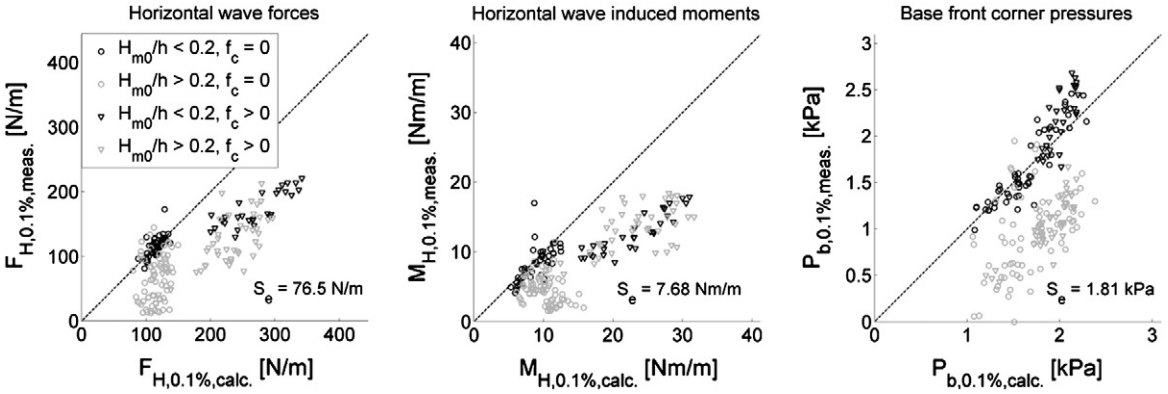


**Fig. 9.** Performance of formulae by Pedersen (1996) in deep and shallow water wave conditions. Data: Present measurements.

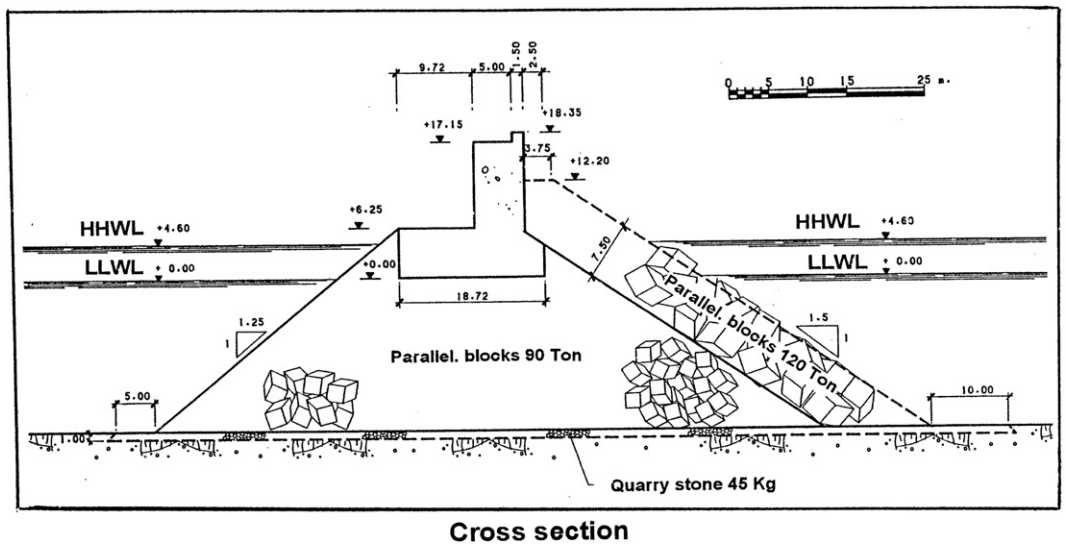


**Fig. 10.** Cross section in prototype scale of the Gijón breakwater tested by Martin et al. (1999).

### 7.2. Update of design formulae for pressures on unprotected wall

Pedersen (1996) used Philips P13-OEM pressure transducers to measure the wave pressures on the superstructure. The pressure transducers, still available in the laboratory at Aalborg University, are from previous experience found to be influenced by dynamic amplification. The amplification is only dominant in case of direct wave slamming on the unprotected part of the superstructure. The Drück PMP UNIK series pressure transducers used in the present tests have a correct frequency response up to 5 kHz and are thus unaffected by dynamic amplifications in the present tested conditions.

Tests in which both the old Philips transducers and the new Drück transducers were installed side by side in the unprotected part of the structure ($f_c > 0$) were performed for comparison. The comparison of the transducers is performed in Fig. 15 for $F_{H,0.1\%}$. Results from deep water wave conditions are shown in the figure.

As seen from Fig. 15 (left), the estimated $F_{H,0.1\%}$ are consistent with the results from the old Philips transducers when using the original empirical factors by Pedersen (1996). However, when comparing against the measurements from the new Drück transducers, the original empirical factors provide an overestimation of $F_{H,0.1\%}$. In Fig. 15 (right), the empirical factor $b$ is fitted to the measurements from the Drück transducers, resulting in the modified factor $b = 1$.

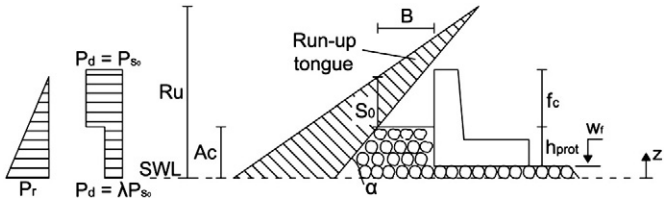


**Fig. 11.** Assumed pressure distribution by Martin et al. (1999).

### 7.3. Update of relation between overturning moment and horizontal wave load

Alternative to the formula by Pedersen (1996) in Eq. (6), $M_{H,0.1\%}$ can be estimated by Eq. (13), based on the pressures on the actual heights $y_{eff}$ and $h_{prot}$, cf. Fig. 8. $e_1$ and $e_2$ are used for calibration of the pressure distribution on the protected and unprotected wall faces, respectively. The calibration factors are determined based on the least square error when fitting to the data. The modified approach is expected to provide better estimates in situations with e.g. $f_c = 0$ since this will lead to an attack point of the resulting $F_H$ at $0.50 \cdot h_{prot}$, which makes sense according to the assumed pressure distribution in

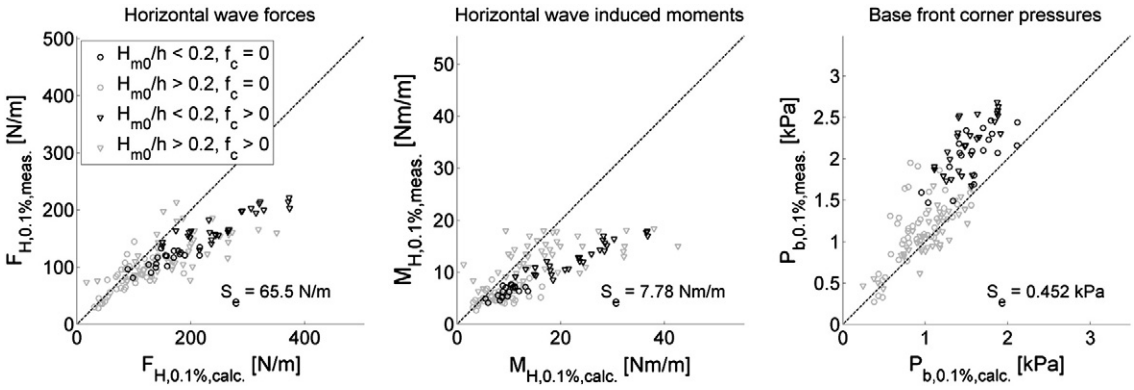


**Fig. 12.** Performance of formulae by Martin et al. (1999) in deep and shallow water wave conditions. Data: Present measurements.

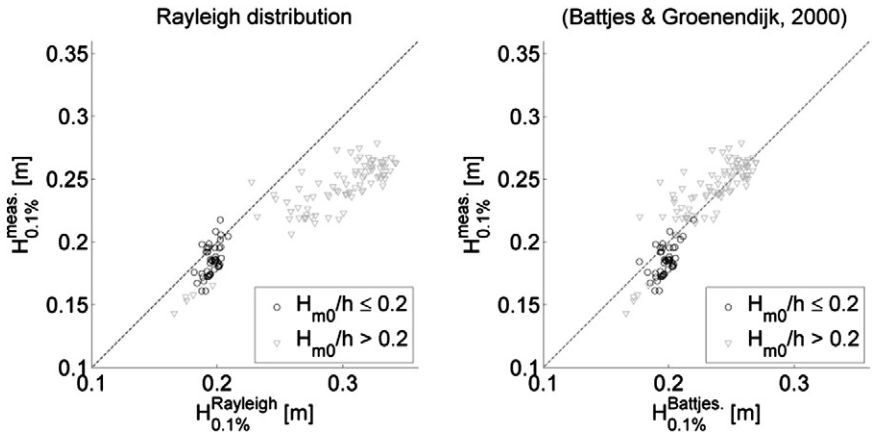


**Fig. 13.** Comparison of measured $H_{0.1\%}$ with predictions based on the Rayleigh distribution and the method of Battjes and Groenendijk (2000). Deep and shallow water wave conditions.

Fig. 8 (left), instead of $0.55 \cdot h_{prot}$ as suggested by Pedersen (1996), cf. Eq. (6).

$$M_{H,0.1\%,\mathrm{mod.}} = \left(h_{prot} + \frac{1}{2}\cdot y_{eff}\cdot e_2\right)\cdot F_{Hu,0.1\%} + \frac{1}{2}\cdot h_{prot}\cdot F_{Hl,0.1\%}\cdot e_1 \qquad (13)$$

The original expression (Eq. (6)) for $M_{H,0.1\%}$ by Pedersen (1996) is compared to the new expression (Eq. (13)) in Fig. 16, using two different ratios between the wave loads on the protected and un-protected parts of the crown wall. The calibration factors are fitted to the data giving $e_1 = 0.95$ and $e_2 = 0.40$. $e_1$ is close to unity which indicates that the assumed constant pressure distribution on the protected wall face is not far off. For the upper wall part there is a significant decrease of pressure with elevation and therefore $e_2$ is significantly lower than unity.

From Fig. 16, it is seen that $M_{H,0.1\%}$ is slightly overestimated for $f_c = 0$ ($F_{Hu,0.1\%}/F_{Hl,0.1\%} = 0$) when using the formula in Eq. (6) compared to the alternative approach in Eq. (13). For higher $F_{Hu,0.1\%}/F_{Hl,0.1\%}$ ratios, the two approaches provide similar results. Additional $F_{Hu,0.1\%}/F_{Hl,0.1\%}$ ratios are evaluated in Table 5 where it is seen that the modified expression in Eq. (13) generally performs better than the original expression for $M_{H,0.1\%}$ in Eq. (6).

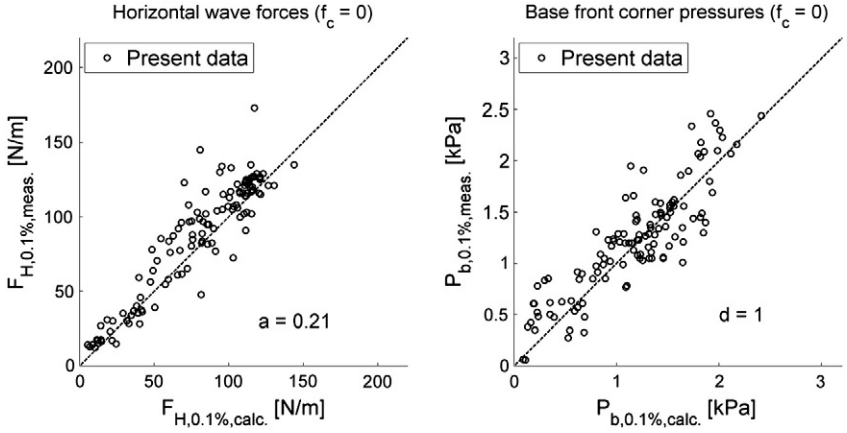


**Fig. 14.** Evaluation of performance of formulae with modified run-up against present measurements ($f_c = 0$).

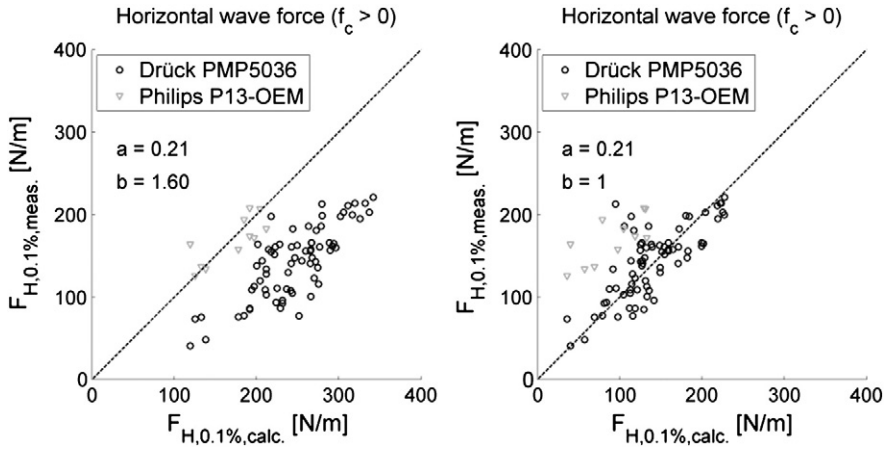


**Fig. 15.** Modification of formulae for $F_{H,0.1\%}$ ($f_c > 0$). (Left) Original formulae by Pedersen (1996). (Right) Modified formulae including modified wave run-up heights and *b*-factor. Data: Present measurements.

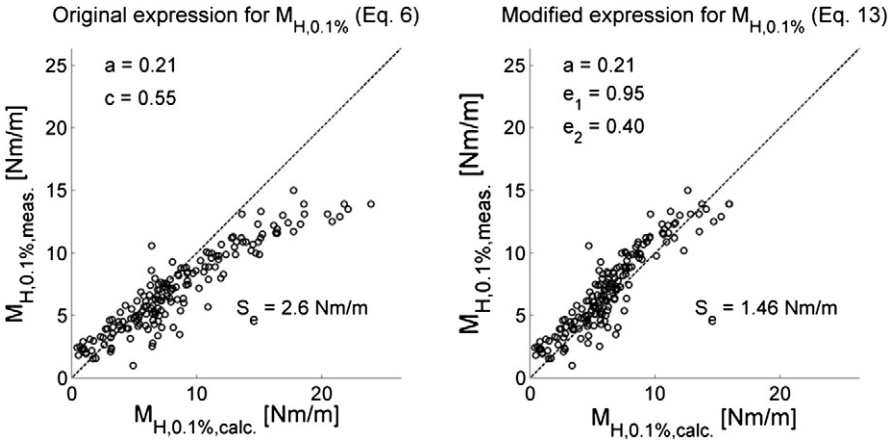


**Fig. 16.** Comparison of original and modified expressions for $M_{H,0.1\%}$ with $F_{Hu,0.1\%}/F_{Hl,0.1\%} = 0$. Data: Present data and data by Pedersen (1996) with $f_c = 0$.

## 8. Evaluation of updated design formulae for loads on superstructures

The modified equations to be used in combination with the modified wave run-up height are summarized in Table 6 together with standard deviations, $\sigma$, and mean values, $\mu$, of the constants.

The performances of the modified formulae and calibration factors are evaluated in Fig. 17. The figure includes the present test data for both deep water waves and shallow water waves and for $f_c \geq 0$ together with the data by Pedersen (1996) for $f_c = 0$.

The evaluated ranges in Fig. 17 are summarized in Table 7. Since the unprotected part of the wall is solely evaluated for the present data set (the modified *b*-parameter), the ranges are divided into ranges for $f_c = 0$ and $f_c > 0$.

It is strictly advised to only apply the modified design formulae within the validated ranges in Table 7. The modified formulae are expected to provide unrealistic results for very low wave steepness; $H_{m0}/L_{m0} < 0.018$.

As mentioned, other run-up formulae than by Van der Meer and Stam (1992) may be applied for estimation of $R_{u,0.1\%}$. However, this may slightly change the empirical parameters derived in the present paper.

## 9. Correlation of maximum load contributions on crown wall

The maximum values of $F_H$, $M_H$, and $P_b$ do not necessarily occur simultaneously. Fig. 18 shows the correlation between the measured maximum values of the base pressures, $P_{b,max}$, and the base pressures

**Table 5**
Performance of the original and modified expressions for $M_{H,0.1\%}$ with various $F_{Hu,0.1\%}/F_{Hl,0.1\%}$ ratios.

| $F_{Hu,0.1\%}/F_{Hl,0.1\%}$ [–] | $S_e$ [Nm/m] (Eq. (7)) | |
|---|---|---|
| | $c = 0.55$ [–] | $e_1 = 0.95$, $e_2 = 0.40$ [–] |
| 0 | 2.64 | 1.46 |
| 0–0.5 | 2.83 | 2.09 |
| 0.5–1 | 5.92 | 5.83 |

**Table 6**
Modified empirical factors and formulae for estimation of wave loads in deep and shallow water wave conditions.

| | |
|---|---|
| Max. wave height, $H_{0.1\%}$ | Measured/Battjes and Groenendijk (2000) |
| Max. wave run-up height, $R_{u,0.1\%}$ | Eq. (12) |
| Max horizontal load, protected wall face, $F_{Hl,0.1\%}$ | Eq. (5), $\sigma_a/\mu_a = 0.06/0.21$ |
| Max horizontal load, un-protected wall face, $F_{Hu,0.1\%}$ | Eq. (5), $\sigma_b/\mu_b = 0.81/1$ |
| Max base pressure, $P_{b,0.1\%}$ | Eq. (6), $\sigma_d/\mu_d = 0.41/1$ |
| Max horizontal moment, $M_{H,0.1\%}$ | Eq. (13), $\sigma_{e1}/\mu_{e1} = 0.53/0.95$, $\sigma_{e2}/\mu_{e2} = 0.78/0.40$. |

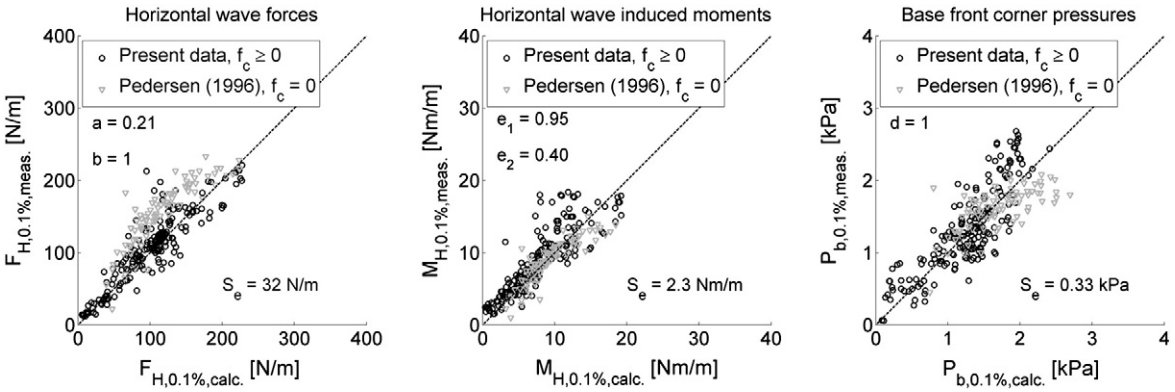


**Fig. 17.** (Left) Modification of formula for $F_{H,0.1\%}$ ($f_c \geq 0$). (Middle) Modification of formula for $M_{H,0.1\%}$ ($f_c \geq 0$). (Right) Modification of formula for $P_{b,0.1\%}$ ($f_c \geq 0$).

**Table 7**
Investigated parameter ranges in modified design-formulae for $F_{H,0.1\%}$, $M_{H,0.1\%}$, and $P_{b,0.1\%}$.

| Parameters | Ranges $f_c = 0$ | Ranges $f_c > 0$ |
|---|---|---|
| $\xi_m$ | 2.3–4.9 | 3.31–4.64 |
| $H_s/A_c$ | 0.5–1.63 | 0.52–1.14 |
| $R_c/A_c$ | 0.78–1 | 1–1.7 |
| $A_c/B$ | 0.58–1.21 | 0.58–1.21 |
| $H_{m0}/h$ | 0.19–0.55 | 0.19–0.55 |
| $H_{m0}/L_{m0}$ | 0.018–0.073 | 0.02–0.041 |

at the instance of maximum horizontal wave load, $P_{b,max,FH}$. The correlation between the moments $M_{H,max}$ and $M_{H,max,FH}$ and the vertical forces $F_{V,max}$ and $F_{V,max,FH}$ is shown as well.

The tendency in Fig. 18 indicates that $P_{b,max}$ and $F_{V,max}$ are significantly larger than $P_{b,max,FH}$ and $F_{V,max,FH}$, which means that conservative estimates of the total load on the superstructure are obtained if full correlation is assumed. A good correlation is, however, seen between $M_{H,max}$ and $M_{H,max,FH}$ as could be expected due to the relation between $F_{H,0.1\%}$ and $M_{H,0.1\%}$ given in Eq. (13).

## 10. Conclusions

A comparison has been made between 2-D model test measurements of wave pressures on crown walls in 162 new tests and estimations by the formulae of Pedersen (1996) and Martin et al. (1999). As a starting point it was concluded that the formulae by Martin et al. (1999) provided the best overall load predictions. However, when separating into deep and shallow water wave conditions, the formulae by Pedersen (1996) provided the best load estimates in deep water conditions, or when the crown wall was fully protected by the armour units. On this basis, it was decided to modify the formulae by Pedersen (1996) to cover shallow water wave conditions. This was done by introducing $H_{0.1\%}$ in the run-up formula by Van der Meer and Stam (1992) instead of $H_{1/3}$ in the set of equations. Moreover, the equations have been modified to more accurately predict both wave slamming pressures on the unprotected part of the wall, and the overturning moment caused by the horizontal wave forces.

## Acknowledgements

The support of the European Commission through FP7.2009-1, Contract 244104—THESEUS ("Innovative technologies for safer European coasts in a changing climate"), is gratefully acknowledged.

## References

Aalborg University, 2010. AwaSys Webpage. http://hydrosoft.civil.aau.dk/AwaSys/index.htm. Department of Civil Engineering, Aalborg University.
Battjes, J.A., Groenendijk, H.W., 2000. Wave height distributions on shallow foreshores. Coastal Engineering 40, 161–182.
Burcharth, H.F., Frigaard, P., Berenguer, J.M., Gonzalez, B., Uzcanga, J., Villanueva, J., 1995. Design of the Ciervana breakwater, Bilbao. In: Telford, T. (Ed.), Proc. 4th Coastal Structures and Breakwaters. Institution of Civil Engineers (Chap. 3.).
Günback, A.R., Ergin, A., 1983. Damage and repair of Antalya harbor breakwater. Proc. Conf. on Coastal Structures, Alexandria, Egypt.
Jensen, O.J., 1984. A Monograph on Rubble Mound Breakwaters. Danish Hydraulic Institute.
Klopman, G., van der Meer, J.W., 1999. Random wave measurements in front of reflective structures. Journal of Waterway, Port, Coastal and Ocean Engineering, ASCE 125 (1), 39–45.

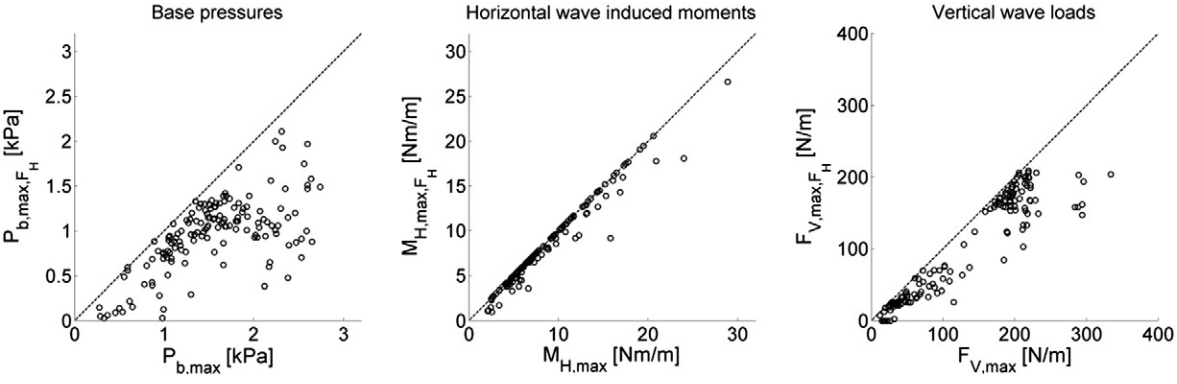


**Fig. 18.** Correlations between the different load parameters on the crown wall.

Kobayashi, N., de los Santos, F.J., Kearney, P.G., 2008. Time-averaged probabilistic model for irregular wave runup on permeable slopes. Journal of Waterway, Port, Coastal and Ocean Engineering, ASCE 134 (2), 88–96.

Lamberti, A., Martinelli, L., Gabriella Gaeta, M., Tirindelli, M., Alderson, J., 2011. Experimental spatial correlation of wave loads on front decks. Journal of Hydraulic Research 2011 (49), 81–90.

Mansard, E.D., Funke, E., 1980. The measurement of incident and reflected spectra using a least square method. Proceedings of the 17th International Conference on Coastal Engineering. ASCE, Vol. 2, pp. 154–172.

Martin, F.L., Losada, M.A., Medina, R., 1999. Wave loads on rubble mound breakwater crown walls. Coastal Engineering 37 (Issue 2), 149–174 (July).

Nørgaard, J.Q.H., Andersen, L.V., Andersen, T.L., Burcharth, H.F., 2012. Displacement of monolithic rubble-mound breakwater crown-walls. 33rd International Conference on Coastal Engineering ICCE 2012, Santander, Spain.

Pedersen, J., 1996. Wave Forces and Overtopping on Crown Walls of Rubble Mound Breakwaters. Ph.D. thesis, Series paper 12, ISBN 0909-4296 Hydraulics & Coastal Engineering Lab., Dept. of Civil Engineering, Aalborg University, Denmark.

U.S. Army Corps of Engineers, 2002. Coastal Engineering Manual. Engineer Manual 1110-2-1100. U.S. Army Corps of Engineers, Washington, D.C.(in 6 volumes).

Van der Meer, J.W., Stam, C.J.M., 1992. Wave run-up on smooth and rock slopes. ASCE, Journal of WPC and OE 188 (No. 5), 534–550 (New York. Also Delft Hydraulics Publication No. 454).